Journal of Power Sources 221 (2013) 78–83

Contents lists available at SciVerse ScienceDirect

Journal of Power Sources

journal homepage: www.elsevier.com/locate/jpowsour

A transparent and stable polypyrrole counter electrode for dye-sensitized solar cell

Chenghao Bu, Qidong Tai, Yumin Liu, Shishang Guo*, Xingzhong Zhao*

School of Physics and Technology, Key Laboratory of Artificial Micro- and Nano-structures of Ministry of Education, Wuhan University, Wuhan 430072, China

HIGHLIGHTS

- A transparent PPy film with electrochemical catalytic activity has been prepared.
- A bifacial DSSC based on this PPy film has been reported for the first time.
- The DSSC based on this PPy counter electrode shows excellent long-term stability.
- The application of this PPy film in DSSC would bring down the production cost.

ARTICLE INFO

Article history:
Received 14 May 2012
Accepted 31 July 2012
Available online 13 August 2012

Keywords:
Transparent polypyrrole counter electrode
In situ preparation method
Bifacial dye-sensitized solar cells
Long term stability
Electrochemical catalytic activity

ABSTRACT

A novel transparent and stable polypyrrole (PPy) electrode that can properly serve as a counter electrode for the bifacial dye-sensitized solar cell (DSSC) has been prepared by in situ polymerization of pyrrole monomer on FTO glass. Cyclic voltammetry (CV) and electrochemical impedance spectroscopy (EIS) measurement show the considerable catalytic activity of PPy counter electrode. The photovoltaic parameters of bifacial DSSCs are strongly dependent on the initial monomer concentration of pyrrole. The optimized PPy counter electrode has been fabricated under the initial monomer concentration of 0.3 M, a bifacial DSSC based on this PPy electrode shows conversion efficiencies of 5.74% and 3.06% corresponding to front- and rear-side illumination, respectively. Compared to the conventional Pt-based DSSCs, the design of bifacial DSSC with transparent PPy counter electrode improves the utilization ratio of incident light. Moreover, the considerable conversion efficiency and the good long-term stability of PPy-based device demonstrated by the stability test highlight the potential large-scale commercial application of this transparent PPy counter electrode.

1. Introduction

As a potential alternative to the traditional silicon-based solar cell, dye-sensitized solar cell (DSSC) has attracted widespread scientific interests due to its low-cost, high conversion efficiency and ease of fabrication [1,2]. A typical DSSC comprises a high surface area dye-sensitized TiO_2 photoanode, a good ion-transporting electrolyte containing a redox couple (I^-/I_3^-) and an efficient counter electrode [3].

Counter electrode (CE) is a critical component of DSSC, which serves as a mediator for collecting electrons from external circuit and reducing I_3^- ions to I^- ions so as to regenerate the redox couple. Platinized counter electrode has been widely used in DSSC so far, due to its high conductivity and catalytic activity for reduction of I_3^- ions. However, platinized CE is restricted by high cost and corrosion of platinum in the presence of I^-/I_3^- redox in electrolyte [4], it is desirable to develop low-cost and more stable materials such as carbon-based materials [5–10] (carbon black, graphite, mesoporous carbon, carbon nanotubes) and conducting polymers including poly(3,4-ethylenedioxythiophene) [11,12] and polyaniline [13,14] as more economic alternatives to platinized CE. As a well known conducting polymer, polypyrrole (PPy) has attracted more and more research interests as a potential candidate for platinized counter electrode because of its facile synthesis, high catalytic activity and considerable environmental stability [15,16].

Recently, the application of spherical PPy as the counter electrode in DSSC had been reported by Jeon et al. [16]. Though a conversion efficiency of 7.7% was obtained, several micrometres thickness of PPy film was required to obtain the desirable catalytic activity and electronic conductivity [6,17]. Therefore, the PPy-based counter electrode they prepared was opaque and unsuitable for

* Corresponding authors. Tel.: +86 27 87642784; fax: +86 27 68752569.
E-mail addresses: gssyhx@whu.edu.cn (S. Guo), xzzhao@whu.edu.cn (X. Zhao).

0378-7753/$ – see front matter © 2012 Elsevier B.V. All rights reserved.
http://dx.doi.org/10.1016/j.jpowsour.2012.07.117

application in bifacial DSSC. To our knowledge, the bifacial DSSC based on transparent CE that can be operated by introducing light from both sides, has the advantage for higher energy production efficiency [18,19]. Moreover, the mechanical stability of the ex-situ prepared PPy CE could be limited for the poor adhesion between PPy film and FTO substrate. Xia et al. have successfully prepared a thin PPy counter electrode by vapour phase polymerization (VPP) [15]. Unfortunately, the conversion efficiency of device based on this thin PPy CE was very low (3.3%). By now, the preparation of PPy film with both high transparency and sufficient electrochemical catalytic activity still remains a challenge.

In this paper, we report on the use of a transparent PPy film as an efficient counter electrode in bifacial DSSC for the first time (as shown in Fig. 1). The PPy CE is prepared by in situ polymerization of pyrrole monomer on FTO glass and the derived photovoltaic parameters of bifacial DSSCs have been optimized by adjusting the initial pyrrole monomer concentrations. The optoelectrochemical properties of PPy film and the stability of sealed bifacial DSSC based on PPy CE have been investigated. Electrochemical measurements display a low charge transfer resistance of 2.46 Ω cm^2 for the PPy CE, which manifests the sufficient catalytic ability for the reduction of I_3^- ions. The high total (the sum of front-and rear-conversion efficiencies) conversion efficiency (8.8%) and the considerable long-term stability of bifacial DSSCs indicate the potential large-scale commercial application of this transparent PPy counter electrode.

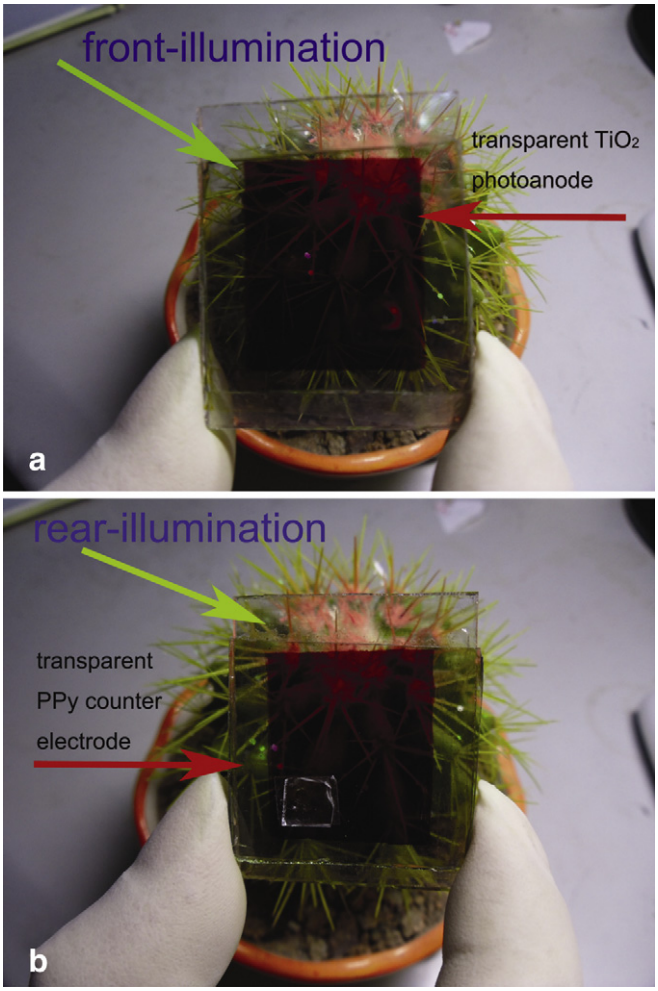

Fig. 1. Digital photographs of the bifacial DSSC employing transparent PPy counter electrode and its operation mode (under front-and rear-illumination).

2. Experimental details

2.1. Preparation of transparent PPy and Pt electrode

In a typical procedure, cetyltrimethylammonium bromide (3.64 g, 10 mM) was first dissolved in 100 mL of 1.0 M HCl solution and then a series of monomer concentrations (0.05 M, 1.0 M, 2.0 M, 3.0 M, 4.0 M) pyrrole were added to the solution with vigorous stirring for 1 h at 0 °C. The resulting viscous mixture was ultrasonicated for 30 min until it became transparent. Then 20 mM ammonium persulfate (APS) was added and the solution turned grey. A piece of well-cleaned FTO glass was immersed in the solution immediately, after being kept at 0 °C for 3 h, the FTO glass was taken out and rinsed with distilled water, the PPy on the nonconductive side was removed. Finally, the PPy/FTO was redoped in 1.0 M HCl for 2 h, and then rinsed and dried at 80 °C for 1 h. The Pt electrode was prepared for comparison by depositing a thin layer of Pt on FTO using magnetron sputtering.

2.2. Assembly of DSSCs

TiO_2 paste was first synthesized by hydrothermal method, then it was doctor-bladed on FTO glass and sintered at 500 °C for 30 min. The procedure was repeated twice. The TiO_2 photoanode was immersed in 50 mM $TiCl_4$ (aqueous) at 70 °C for 30 min and then sintered at 500 °C for 30 min. The resulting TiO_2 photoanode was then immersed in an acetonitrile solution containing 0.5 mM N_3 dye and kept at 60 °C for 12 h. The DSSC was assembled by a sandwiching process: the dye-absorbed TiO_2 photoanode was tightly clipped with PPy or Pt counter electrode, a drop of liquid electrolyte containing 1 M PMII (1-methyl-3-propyl imidazolium iodide), 0.04 M LiI, 0.03 M I_2, 0.1 M GuSN (guanidinium thiocyanate), 0.5 M TBP (4-tert-butylpyridine) in acetonitrile and propylene carbonate ($v/v = 1{:}1$) was added to fill the void between two electrodes by the capillary effect.

2.3. Characterization

UV–visible transmitted spectra of the PPy films were recorded on UV/VIS spectrometer (Lambda 650S Perkin Elmer). The morphologies of the PPy film on FTO glass was observed by scanning electron microscopy (SEM, JEOL, 6700F, Japan) and atomic force microscopy (AFM, SPM9500J3, Shimadzu, Japan). Cyclic voltammetry was performed on CHI 660C (Shanghai, China) electrochemical station with a Pt plate as auxiliary electrode, an Ag/Ag^+ electrode as reference electrode, and a PPy/FTO or a Pt/FTO electrode as working electrode in an acetonitrile solution containing 10 mM LiI, 1 mM I_2 and 0.1 M $LiClO_4$ as supporting electrolyte. Electrochemical impedance spectroscopy (EIS) of the PPy and Pt counter electrodes was also performed on CHI 660C with the frequency from 100 kHz to 0.1 Hz. For the EIS measurement, a symmetric cell configuration with two identical PPy or Pt CEs was assembled with the injection of the same electrolyte for the DSSCs, and the active area of the cells was controlled at 0.25 cm^2 by Surlyn. The photocurrent density–voltage (J–V) characteristics were measured under AM 1.5 simulated illumination with a power density of 80 mW cm^{-2}, the active area was controlled at 0.25 cm^2 by a mask.

3. Results and discussion

Fig. 2 shows the UV–visible transmitted spectra of transparent PPy electrodes prepared under different pyrrole monomer concentrations (Py MC). The thin PPy film on FTO glass shows excellent transparency range from 300 nm to 800 nm. The

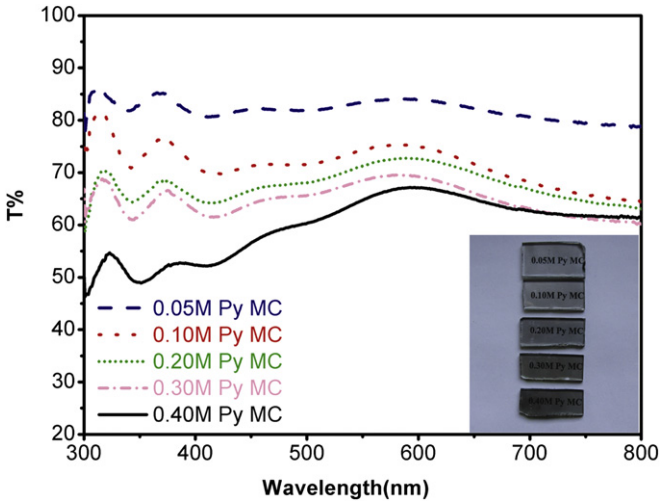

Fig. 2. UV–visible transmitted spectrum of the PPy counter electrodes prepared by polymerizing pyrrole on FTO glass under different initial monomer concentrations (the pure FTO glass was used as the reference).

absorption of N3 dye is mainly in the range of 450 nm–600 nm [18], so the transmittance of PPy in this range is of research interest. It is found that the transmittance of PPy film on FTO glass increases with the decrease of pyrrole monomer concentration, which is beneficial for bifacial illumination of DSSCs. The inset in Fig. 2 gives the demonstration of transparent PPy CEs prepared under different pyrrole monomer concentrations. It is observed that the PPy film becomes transparent gradually by decreasing monomer concentrations of pyrrole and the incident light can penetrate from the rear side of the DSSC more easily.

The *J–V* curves of devices employing PPy CEs prepared under different pyrrole monomer concentrations (0.05, 0.1, 0.2, 0.3, 0.4 M) are shown in Fig. 3a (under front-illumination, AM 1.5, 80 mW cm^{-2}) and Fig. 3b (under rear-illumination, AM 1.5, 80 mW cm^{-2}). The derived photovoltaic parameters are summarized in Table 1. It is found that when irradiated from the front side, the short circuit current density (J_{sc}) of device based on PPy CE increases with the increase of pyrrole monomer concentration and the conversion efficiency consequently increases as a result of J_{sc} increase. This phenomenon can be attributed to the fact that the catalytic activity of PPy CE keeps growing with the increase of pyrrole monomer concentration. However, when irradiated from the rear side, the variation tendencies of J_{sc} and conversion efficiency are irregular with the increase of pyrrole monomer concentration, which are the compromise of the increased catalytic activity and the reduced transparency of the PPy film as the pyrrole monomer concentration increased. The total (the sum of front- and rear-illumination conversion efficiencies) conversion efficiencies of DSSCs based on PPy CEs prepared under different pyrrole monomer concentrations are shown in Fig. 3c. The device gives the optimal η of 5.74% under front-illumination and η of 3.06% under rear-illumination when the initial monomer concentration is 0.3 M. Therefore, the optimized monomer concentration of 0.3 M has been obtained and will be used for following investigation.

Fig. 4 shows the SEM surface morphologies of FTO glass and in situ prepared (0.3 M pyrrole monomer concentration) PPy film. The bare FTO surface shows the characteristic morphology of tin oxide crystals with compact rod-shaped grains around 250 nm (Fig. 4a). When the PPy is deposited, the film exhibits porous structure with cotton-shaped grains (Fig. 4b). A more detailed AFM image presented in Fig. S1 shows that these cotton-shaped grains are composed of smaller particles around 40 nm. The root mean square

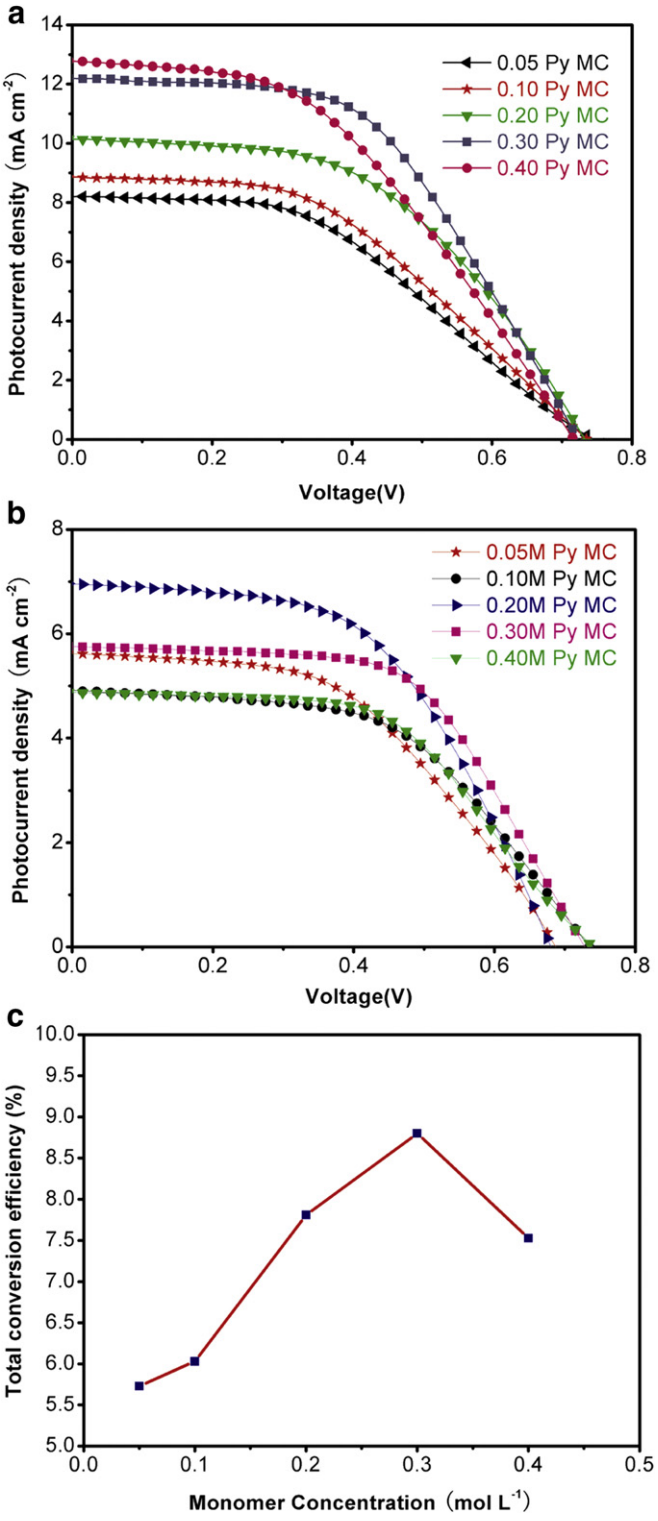

Fig. 3. (a) *J–V* curves of DSSCs fabricated with different PPy-CEs under front-illumination. (b) *J–V* curves of DSSCs fabricated with different PPy-CEs under rear-illumination. (c) The sum of front-and rear-illumination conversion efficiencies of DSSCs fabricated with PPy-CEs prepared under various monomer concentrations ($\eta_f + \eta_r$).

(rms) roughnesses of the FTO and PPy film calculated from AFM are 17.9 nm and 25.9 nm, respectively (see Table S1). The increased roughness reveals that the porous structure of PPy film will render it with high surface area, which enhances the tri-iodide diffusion efficiency [7,20].

Table 1
Photovoltaic parameters of bifacial DSSCs based on PPy-CEs prepared from various monomer concentrations of pyrrole.

Monomer concentration [mol L^{-1}]	Front-illumination (rear-illumination)			
	V_{oc} [mV]	J_{sc} [mA cm $^{-2}$]	FF	η [%]
0.05	745 (685)[a]	8.20 (5.62)	0.44 (0.50)	3.34 (2.39)
0.10	735 (735)	8.86 (4.91)	0.45 (0.53)	3.63 (2.40)
0.20	735 (715)	10.14 (6.95)	0.50 (0.53)	4.68 (3.13)
0.30	725 (725)	12.19 (5.75)	0.52 (0.58)	5.74 (3.06)
0.40	715 (735)	12.72 (4.87)	0.44 (0.55)	5.02 (2.46)

Note: The parameters were measured under 80 mW cm^{-2}, AM 1.5 simulated irradiation. The active area was 0.25 cm^2.
[a] The parameters measured under the rear-illumination (shown in parentheses).

Cyclic voltammetry (CV) was applied to investigate the reaction kinetics of various electrodes in the electrochemical system. Fig. 5 shows the CV curve of PPy CE (prepared under 0.3 M pyrrole monomer concentration), the Pt CE had been investigated under the same conditions for comparison. The two pairs of redox waves observed represent the oxidation and reduction of I^-/I_3^- (the left pair) and I_2/I_3^- (the right pair). The counter electrode in a DSSC serves to catalyse the reduction of I_3^- to I^-, thus the characteristics of the left pair are our research focus [21,22]. The PPy CE exhibits higher peak current density than that of Pt CE, which manifests a faster reaction rate of I_3^- reduction on the PPy film, thus a higher apparent catalytic activity of PPy CE [14,23], which is advantageous for the application of PPy as an efficient counter electrode in DSSCs.

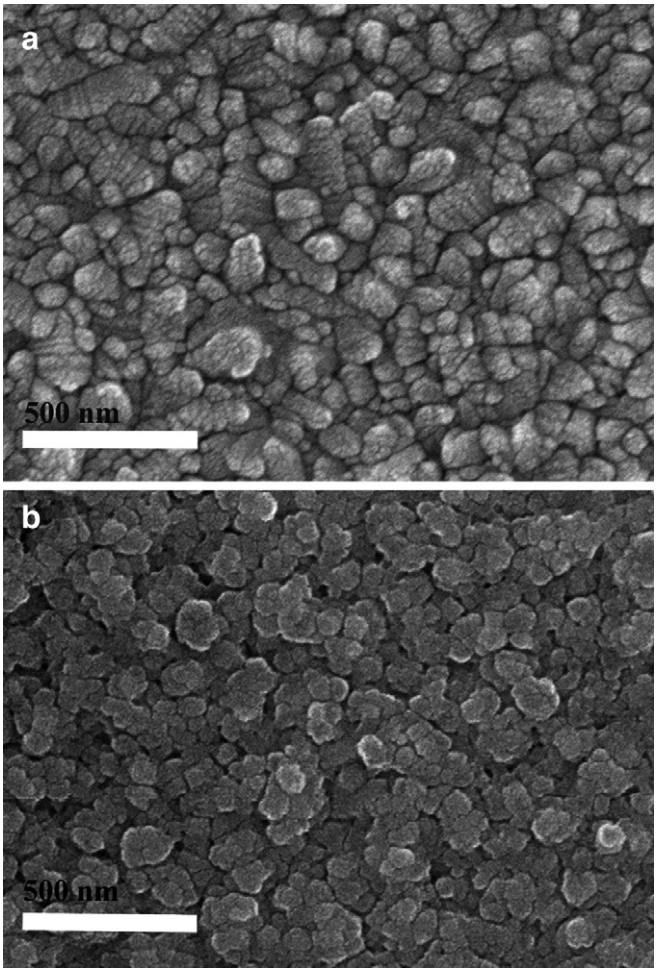

Fig. 4. The SEM images of the FTO and PPy film prepared under 0.3 M pyrrole monomer concentration: (a) FTO; (b) PPy film on FTO.

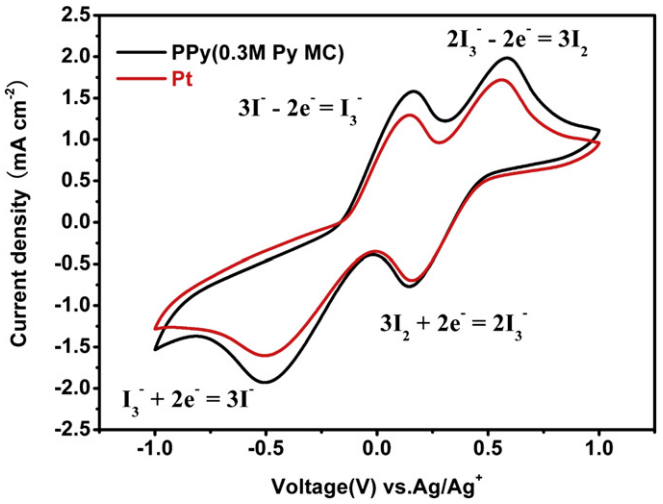

Fig. 5. Cyclic voltammetry for PPy-CE and Pt-CE obtained at a scan rate of 50 mV s^{-1} in a 10 mM LiI, 1 mM I_2 acetonitrile solution containing 0.1 M $LiClO_4$ as the supporting electrolyte.

In order to examine the electrochemical characteristics of PPy and Pt CEs, electrochemical impedance spectroscopy (EIS) was conducted. The symmetrical PPy–PPy and Pt–Pt electrochemical cells were made by assembling two identical PPy (or Pt) CEs on each side separated by a spacer containing an electrolyte used in full functional DSSCs [24]. These two symmetrical cells were used for EIS measurement to eliminate the influence of photoanode. Fig. 6 shows the Nyquist plots of the symmetrical PPy–PPy and Pt–Pt electrochemical cells. The interpretation of such EIS spectrum has been well-established [24–26]: the intersection of high frequency semicircle at real axis represents ohmic series resistance of device

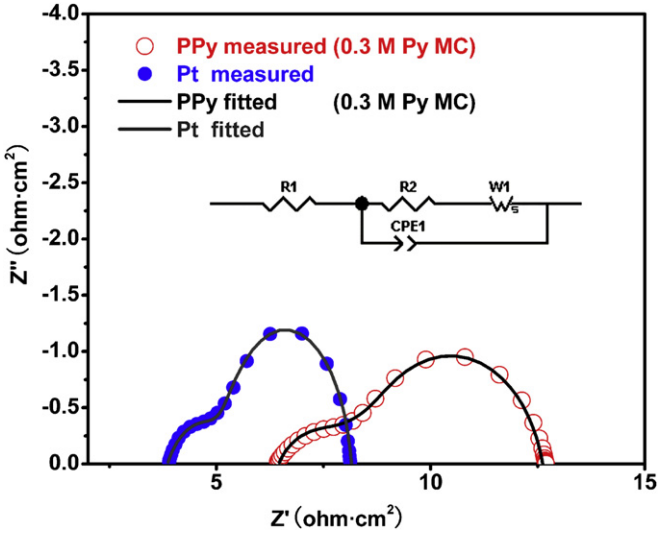

Fig. 6. Nyquist plots of the symmetrical cells consisting of two identical PPy and Pt electrodes. The inset is the equivalent circuit of the symmetrical PPy–PPy or Pt–Pt electrode electrochemical cell for EIS measurement. R1: ohmic series resistance of the symmetrical cell (R_s); R2: the charge transfer resistance (R_{ct}) at the electrode/electrolyte interface; CPE1: Constant phase element (capacitance at the electrode/electrolyte interface); W1: Nernst diffusion impedance (Z_w) of the I^-/I_3^- redox couple in a thin layer of electrolyte. The symbols represent the experimental data and the solid lines represent the fitting results.

Table 2
The fitted EIS parameters of the symmetrical cells with PPy and Pt electrodes.

Samples	R_s (Ω cm^{-2})	R_{ct} (Ω cm^{-2})
PPy electrode (0.3 M Py MC)	6.5	2.46
Pt electrode	3.8	2.53

(R_s); the diameter of high frequency semicircle represents the charge transfer resistance (R_{ct}) at the electrode/electrolyte interface, while the low frequency arc is attributed to the Nernst diffusion impedance (Z_W) of the I^-/I_3^- redox couple in a thin layer of electrolyte. The Nyquist plots have been fitted with the inset equivalent circuit and the results are shown in Table 2. The CPE represents the capacitance at the interface between the electrode and electrolyte. The R_{ct} of PPy electrode is found to be 2.46 Ω cm^2, which is comparable to that of Pt (2.53 Ω cm^2), indicating the similar intrinsic catalytic activities for the reduction of I_3^- on PPy electrode surface. The higher apparent catalytic activity of PPy film observed in CV measurement is attributed to its larger effective surface area as revealed by the AFM characterization (see Fig. S1 and Table S1). However, the R_s of PPy symmetrical cell is 6.5 Ω cm^2, which is larger than that of Pt symmetrical cell (3.8 Ω cm^2), displaying a higher sheet resistance of PPy electrode. The large R_s can affect the fill factor (FF) of the DSSC based on PPy CE [27], and it will be interpreted in the following section.

Fig. 7 shows the representative *J–V* characteristics of the bifacial DSSC employing transparent PPy CE under front- and rear-illumination (AM 1.5, 80 mW cm^{-2}). The device based on Pt CE also has been measured under the same conditions. The derived photovoltaic parameters are summarized in Table 3. When irradiated from the front side, the device exhibits a short circuit current density (J_{sc}) of 12.19 mA cm^{-2}, an open circuit voltage (V_{oc}) of 725 mV, and a fill factor (FF) of 0.52, resulting in a conversion efficiency (η) of 5.74%, which approaches 80% of the device with Pt electrode (6.76%).

It is found that the J_{sc} of the device with PPy CE (12.19 mA cm^{-2}) is higher than that of Pt CE (10.45 mA cm^{-2}). The enhanced J_{sc} may be owing to the higher apparent catalytic activity for the reduction of I_3^- on PPy electrode as confirmed by CV and AFM measurements. The efficiency loss of device based on PPy electrode is attributed to the lower FF (0.52) compared to the Pt electrode (0.70). The FF can

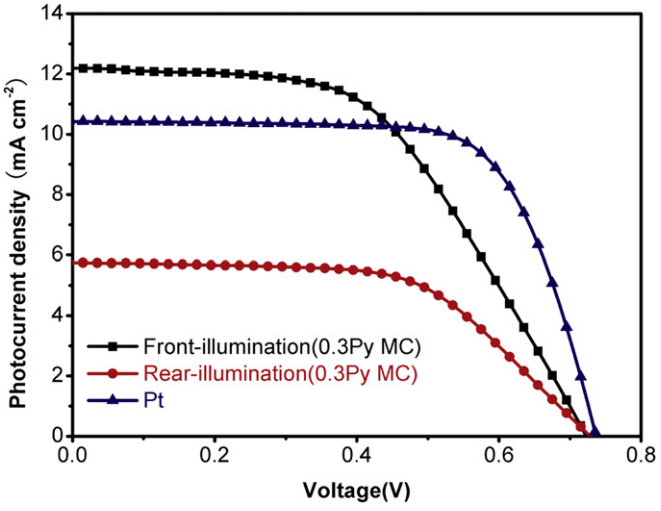

Fig. 7. *J–V* characteristics of DSSCs employing Pt and PPy (prepared under 0.3 M pyrrole monomer concentration) counter electrodes measured under AM 1.5, 80 mW cm^{-2} front-and rear-illumination. The active area is 0.25 cm^2.

Table 3
J–V characteristics of DSSCs based on transparent PPy-CE and Pt-CE measured under 80 mW cm^{-2}, AM 1.5 simulated irradiation with an active area of 0.25 cm^2.

CEs		V_{oc} (mV)	J_{sc} (mA cm^{-2})	FF	η (%)
PPy	Front-illumination	725	12.19	0.52	5.74
	Rear-illumination	725	5.75	0.58	3.06
Pt		735	10.45	0.70	6.76

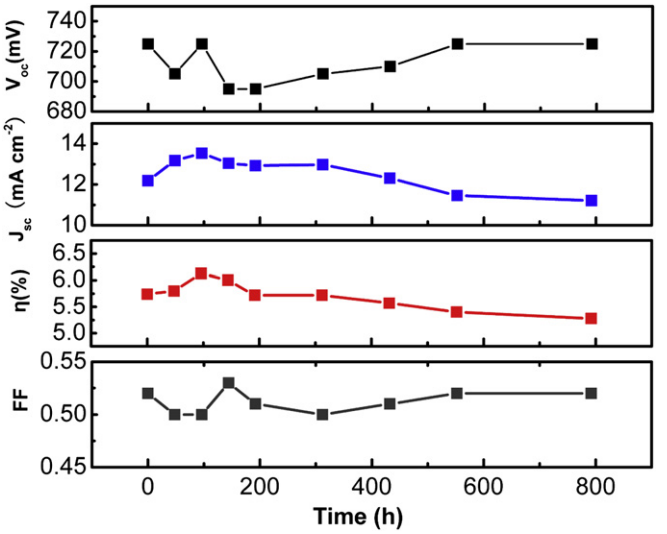

Fig. 8. Time-course changes of the photovoltaic parameters of a sealed DSSC with PPy-CE. The device was kept under the ambient conditions and the data were obtained under AM 1.5 front-illumination (80 mW cm^{-2}) with an active area of 0.25 cm^2.

be affected by the R_s of the device, which has been discussed in EIS characterization. When the light casted from the rear side, the device based on PPy electrode shows lower J_{sc} (5.75 mA cm^{-2}) and η (3.06%), but higher FF (0.58) compared to the front-illumination. The reduction of J_{sc} and the enhancement of FF are due to the reduced light intensity cast on dye-sensitized TiO_2 resulting from the lower transmittance of PPy film compared to the FTO glass. The relationship between the light intensity and photovoltaic parameters has been well interpreted in elsewhere [28].

To investigate the stability of PPy CEs in DSSCs, a cell was sealed with Surlyn, and the electrolyte was introduced through the drilled hole on the counter electrode. The stability of the device was demonstrated by obtaining photovoltaic parameters several times during a period of 792 h. Fig. 8 shows the evolution of photovoltaic parameters with time for the sealed cell based on PPy CE. From 0 to 96 h, the J_{sc} and conversion efficiency of DSSC increases slightly (from 12.19 mA cm^{-2} to 13.53 mA cm^{-2} and 5.74 % to 6.13 %, respectively), we attribute it to the slow stabilization of electrolyte additives on PPy CE [29]. After 792 h, the device maintains 92% J_{sc} (11.21 mA cm^{-2}) and 90% conversion efficiency (5.28%), the V_{oc} and FF show negligible variation, it reveals that the series resistance of device remains stable and PPy electrode exhibits considerable long-term stability because of the good connection between the PPy film and the FTO glass.

4. Conclusion

In summary, a novel transparent PPy CE has been prepared by in situ polymerization of pyrrole on FTO glass. The PPy CE exhibits sufficient apparent catalytic activity towards the reduction of I_3^- due to the porous structure of PPy film with high surface area. The

excellent transparency of PPy film in visible region allows PPy-CE based DSSCs to be operated by introducing light from both sides, thus enhancing the light utilization efficiency. The optimized conversion efficiency of 5.74% (under front-illumination) and 3.06% (under rear-illumination) have been obtained by employing PPy CE prepared under 0.3 M pyrrole monomer concentration. Moreover, the PPy CE based DSSC shows good long-term stability owing to the strong connection between in situ prepared PPy film and the FTO substrate. The facile polymerization procedure, excellent transparency, low cost and good stability enable this PPy film to be a promising alternative counter electrode in large-scale production of bifacial DSSCs.

Acknowledgements

We gratefully acknowledge the financial support of this work by the National Basic Research Program (No. 2011CB933300) of China and the National Science Fund for Talent Training in Basic Science (Grant No. J0830310).

Appendix A. Supporting information

Supporting information related to this article can be found at http://dx.doi.org/10.1016/j.jpowsour.2012.07.117.

References

[1] B. O'Regan, M. Gratzel, Nature 353 (1991) 737–739.
[2] M. Gratzel, Nature 414 (2001) 338–344.
[3] Jinkyu Han, Hyunju Kim, Dong Young Kim, Seong Mu Jo, Sung-Yeon Jang, ASC Nano. 4 (2010) 3503–3509.
[4] Takurou N. Murakami, M. Gratzel, Inorg. Chim. Acta 361 (2008) 572–580.
[5] A. Kay, M. Gratzel, Sol. Energy Mater. Sol. Cells 44 (1996) 99–117.
[6] K. Suzuki, M. Yamaguchi, M. Kumagai, S. Yanagida, Chem. Lett. 23 (2003) 28–29.
[7] G. Wang, Wei Xing, Shuping Zhuo, J. Power Sources 194 (2009) 568–573.
[8] Seung I. Cha, B.K. Koo, S.H. Seo, Dong Y. Lee, J. Mater. Chem. 20 (2010) 659–662.
[9] Prakash Joshi, Yu Xie, Mike Ropp, David Galipeau, Shelia Bailey, Qiquan Qiao, Energy Environ. Sci. 2 (2009) 426–429.
[10] S.C. Feng, L. Jing, L.T. Zhan, C. Jun, S.X. Rui, J. Power Sources 177 (2008) 631–636.
[11] J.B. Xia, N. Masaki, K.J. Jiang, S. Yanagida, J. Mater. Chem. 17 (2007) 2845–2850.
[12] S. Ahmad, J.H. Yum, X.X. Zhang, M. Gratzel, H.J. Butt, J. Mater. Chem. 20 (2010) 1654–1658.
[13] Zuopeng Li, Baoxi Ye, Xiaodong Hu, Xiangyuan Ma, Xiaoping Zhang, Youquan Deng, Electrochem. Commun. 11 (2009) 1768–1771.
[14] Huicheng Sun, Yanhong Luo, Yiduo Zhang, Dongmei Li, Zhexun Yu, Kexin Li, Qingbo Meng, J. Phys. Chem. C 114 (2010) 11673–11679.
[15] Jiangbin Xia, Lingchen, Shozo Yanagida, J. Mater. Chem. 21 (2011) 4644–4649.
[16] Sang Soo Jeon, Chulwoo Kim, Jaejung Ko, Seung Soon Im, J. Mater. Chem. 21 (2011) 8146–8151.
[17] T.N. Murakami, S. Ito, Q. Wang, M.K. Nazeeruddin, T. Bessho, I. Cesar, P. Liska, R. Humphry-Baker, P. Comte, P. Péchy, M. Grazel, J. Electrochem. Soc. 153 (2006) A2255–A2261.
[18] Qidong Tai, Bolei Chen, Feng Guo, Sheng Xu, Hao Hu, Bobby Sebo, Xing-Zhong Zhao, ACS Nano. 5 (2011) 3795–3799.
[19] S. Ito, Shaik M. Zakeeruddin, P. Comte, P. Liska, D. Kuang, M. Gratzel, Nat. Photonics 2 (2008) 693–698.
[20] Rongrong Jia, Jiazang Chen, Jianghong Zhao, Jianfeng Zheng, Chang Song, Li Lia, Zhenping Zhu, J. Mater. Chem. 20 (2010) 10829–10834.
[21] Q.H. Li, J.H. Wu, Q.W. Tang, Z. Lan, P.J. Li, J.M. Lin, L.Q. Fan, Electrochem. Commun. 10 (2008) 1299–1302.
[22] J. Zhang, Tubshin Hreid, X.X. Li, W. Guo, L.P. Wang, X.T. Shi, H.Q. Su, Z.B. Yuan, Electrochim. Acta 55 (2010) 3664–3668.
[23] Shengjie Peng, Lingling Tian, Jing Liang, Subodh G. Mhaisalkar, Seeram Ramakrishna, ACS Appl. Mater. Interf. 4 (2012) 397–404.
[24] Prakash Joshi, Lifeng Zhang, Qiliang Chen, David Galipeau, Hao Fong, Qiquan Qiao, ACS Appl. Mater. Interf. 2 (2010) 3572–3577.
[25] Anneke Hauch, Andreas Georg, Electrochim. Acta 46 (2001) 3457–3466.
[26] Motonari Adachi, Masaru Sakamoto, Jinting Jiu, Yukio Ogata, Seiji Isoda, J. Phys. Chem. B 110 (2006) 13872–13880.
[27] Qing Wang, Jacques-E. Moser, Michael Gratzel, J. Phys. Chem. B 109 (2005) 14945–14953.
[28] Janne Halme, Paula Vahermaa, Kati Miettunen, Peter Lund, Adv. Mater. 22 (2010) E210–E234.
[29] Hao Hu, Bolei Chen, Chenghao Bu, Qidong Tai, Feng Guo, Sheng Xu, Junhua Xu, Xingzhong Zhao, Electrochim. Acta 56 (2011) 8463–8466.